



This item was submitted to Loughborough's Institutional Repository (<https://dspace.lboro.ac.uk/>) by the author and is made available under the following Creative Commons Licence conditions.


C O M M O N S D E E D

Attribution-NonCommercial-NoDerivs 2.5

You are free:

- to copy, distribute, display, and perform the work

Under the following conditions:

 **Attribution.** You must attribute the work in the manner specified by the author or licensor.

 **Noncommercial.** You may not use this work for commercial purposes.

 **No Derivative Works.** You may not alter, transform, or build upon this work.

- For any reuse or distribution, you must make clear to others the license terms of this work.
- Any of these conditions can be waived if you get permission from the copyright holder.

Your fair use and other rights are in no way affected by the above.

This is a human-readable summary of the [Legal Code \(the full license\)](#).

[Disclaimer](#) 

For the full text of this licence, please go to:
<http://creativecommons.org/licenses/by-nc-nd/2.5/>

Limitations of functionally determined joint centres for analysis of athletic human movement: A case study of the upper limb

Andy Roosen¹, Matthew T.G. Pain¹ and Mickaël Begon²

¹School of Sports and Exercise Sciences, Loughborough University, LE11 3TU, UK

²University of Montreal and Saint-Justine Hospital, Montreal, Canada

ABSTRACT

Much research is ongoing into improving the accuracy of functional algorithms to determine joint centres (JC), but there has been limited testing using human movement data. This paper is in three parts: Part 1, errors in determining JCs from real human movement data using the SCoRE method; Part 2, variability of marker combinations during a punch; Part 3, variability in the JC due to reconstruction. Results indicate determining the JC of the shoulder or elbow with a triad of markers per segment with an accuracy greater than 20 mm is unlikely. Part 2 suggests conducting a pilot study with abundant markers to obtain triads which are most stable due to differences of 300 to 400% in variability between triads. Variability due to the choice of reference frame for reconstruction during the punch ranged from 2.5 to 13.8 mm for the shoulder and 1.5 to 21.1 mm for the elbow. It would appear pertinent to enhance the practical methods *in situ* than to further improve theoretical accuracy of functional methods.

Keywords: 3D motion analysis, instant centre of rotation, functional methods

INTRODUCTION

Human movement analysis is carried out on many scales, ranging from precise clinical joint analysis to technical analysis of explosive sporting movements. An initial step for analysing human movement is the determination of joint centre (JC) locations. Once JC locations have been determined a method of reconstructing them during the movement of interest is normally required. This involves expressing the JC location in terms of a local reference frame of markers on a segment.

The accuracy of functional methods in determining the optimised centres of rotation (OCR) has been tested using computer simulation models and/or rigid mechanical linkage devices (Ehrig et al., 2006; Camomilla et al., 2006; Piazza et al., 2001) and has been shown to approximate OCR to within 1 mm. Although noise is introduced in these models it is pertinent to explore how functional methods perform when implemented on actual human movement data. This has been done in only a few studies and only for the hip and shoulder joints (Monnet et al., 2007; Leardini et al., 1999; Bao & Willems, 1999; Shea et al., 1997). Leardini et al. (1999) found that their functional method approximated the real JC obtained through roentgen stereophotogrammetric analysis better than predictive methods, 13 mm rather than 25 mm (Bell et al., 1990). Monnet et al. (2007) compared the SCoRE method (Ehrig et al., 2006) to the helical axis method in locating the glenohumeral joint *in vivo* and found the former to be more precise and unaffected by movement velocity. However, researchers have warned that implementing functional methods under 'suboptimal' conditions may lead to inaccurate estimation of the OCR (Piazza et al., 2004). Results depend on the type of movement used and the range of motion (RoM) of the joint (Begon et al. 2007; Camomilla et al.,

2006; Siston & Delp, 2006). The RoM really needs to exceed 15° (Camomilla et al., 2006; Piazza et al., 2001) and a marked improvement in accuracy is obtained with a RoM above 20° or in some cases 45° (Ehrig et al., 2006). Further factors that affect the results are the sample number, the proximity of the marker centroid to the actual joint centre, the distance between markers (Camomilla et al., 2006) and the signal processing (Begon et al., 2007; Chèze, 1995). It is also pertinent to remember that although the theoretical literature on functional methods is split into hinge and ball and sockets joints the elbow, knee or ankle are neither truly hinge nor ball and socket joints. The movements performed in the above *in vivo* experiments are limited to determining the JC. They do not explore the limitations of implementing and reconstructing the obtained JC during further movement analysis.

Much research has been done and is still ongoing to improve the accuracy of functional algorithms which determine OCR. However, there is a lack of research in whether the obtained locations can be used accurately and effectively when analysing subsequent human movement, especially where the noise from soft tissue deformation is substantially different from the trials used to determine the OCR. This will be particularly problematic during whole body athletic movements as a number of issues need to be considered. These include: ten-fifteen segments are required to represent the human body; too many markers can inhibit the movement; marker placement will need to be adjusted between subjects as musculature and movement technique may differ; the nature of the athletic movement will cause skin movement artefacts much greater than in simple movements used to approximate JCs.

Once the JCs have been determined the following procedures are commonly performed to allow the reconstruction of JCs during the performance trials and each procedure has limitations associated with it. The OCR is expressed in terms of reference frames representing adjacent segments. These segments will normally be defined using at least three markers for each segment, if the segment motion is to be independently determined. The OCR is expressed as a constant vector in this local reference frame, which assumes that the segment is rigid. This assumption is obviously incorrect as the markers defining the segment will demonstrate movement artefacts (Reinschmidt, 1997; Capozzo, 1996; Karlsson, 1994; Woltring, 1991). Hence, the OCR location will be subject to the variability of the created reference system. This variability may be minimised by using more than three markers, and clusters of markers with optimisation procedures to minimise deformation, but cannot be eliminated fully (Challis, 1995; Andriacchi, 1998).

The first aim of this study is to obtain JC coordinates from human motion data using the method for the upper limb at both the shoulder and elbow and to assess to what degree these locations SCoRE can be estimated *in vivo*. The SCoRE method was chosen as Ehrig al. (2006) had shown that it performed well in comparative tests on models and it also produces large numbers of potential JC for a given number of markers. These comparisons were limited to simulated motion, only a few comparative studies on live human motion exist (Monnet et al., 2007), and other tests performed as well in certain conditions. Given that the elbow joint is neither a hinge or ball and socket joint and in this dynamic task a large amount of pronation and supination were to be expected the SCoRE method was applied to the elbow joint. The second aim is to address potential issues with implementing these JC locations for the analysis of human movement during athletic activities. The second aim should illustrate that despite the theoretically high degree of accuracy of the functional method, the method of recalling the JC location will determine the final accuracy of any movement analysis during such activities.

METHODS

This study was divided into three parts. Part 1 determined JCs based on real human movement data. Part 2 investigated variability of marker combinations from Part 1 during a punch. Part 3 then investigated how the reconstruction of a chosen JC during a punch affected its position. All data were collected at 240 Hz. The algorithms used in each of these three parts are in Appendix 1.

One healthy male volunteer (age: 35; height: 1.75 m; weight: 92 kg), who had given informed consent in accordance with the university's ethical advisory committee procedures took part in this study. The subject was fitted with six retro-reflective markers on each of the following segments: torso, (including the shoulder area), upper arm and forearm (Figure 1).

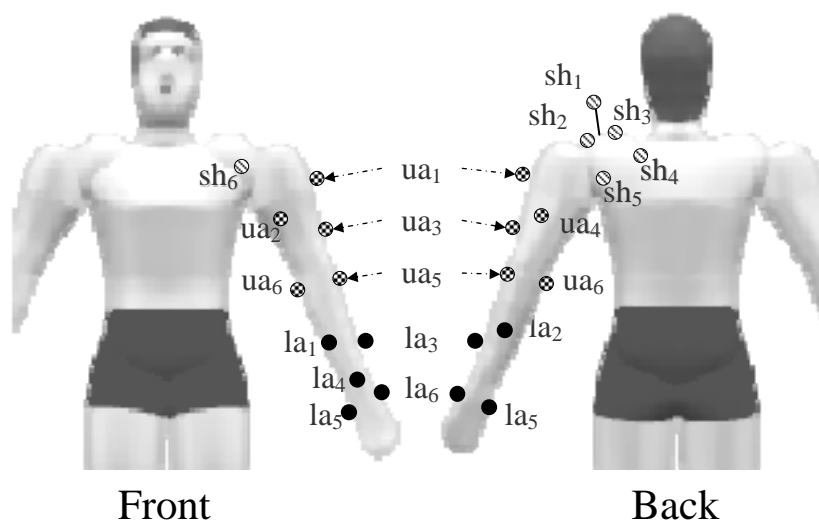


Figure 1: Rear view and front view of the 18 marker locations (six lower arm, six upper arm and six shoulder), each marker is only represented once.

For Parts 1 and 2 all calculations were performed on the raw data and the same data which had undergone solidification using the method proposed by Chèze (1995). In Part 3 only solidified data were analysed.

Part 1

Set-up movement data were collected to determine the locations of the JC. The subject was instructed to perform slow movements over a large range of motion. For the shoulder joints, the subjects performed a star-arc movement (Camomilla et al., 2006). For the elbow, lower arm flexion, extension, pronation, supination and circumduction were performed. During these movements the lower arm motions were carried out with the elbow and shoulder fixed in a global position, as far as was possible. The markers on the lower-arm describe quite decent sectors of a sphere relative to the upper-arm. Given the local frame representation these marker motions are due to the combination of flexion-extension and pronation-supination of the lower arm relative to the upper arm. However, there may also be a contribution from internal-external rotation of the humerus that has not been expressed fully at the upper arm markers due to significant skin movement artefact. The shoulder and elbow set-up movements were acquired at 240 Hz but only every 4th sample was used to reduce the volume of data to 1480 and

1289 samples respectively. Groups of three markers that were used to define a local reference frame were called triads.

Multiple JCs were estimated from the set-up movement data using the SCoRE method (Ehrig et al., 2006) for all permutations of three from six markers in the proximal segment and three from six markers in the distal segment. The SCoRE method determines JC locations relative to each segment which are then combined to reconstruct JCs in the global frame, this yielded ${}^6P_3 \times {}^6P_3 = 14,400$ possible JC locations. All these solutions were reconstructed in a global frame for one time frame of the static trial. The radius of a sphere of 95% confidence and a mean JC location were obtained by iteratively discarding outliers. As the SCoRE method of calculating the JC has been shown to be accurate in theoretical experiments (Ehrig et al., 2006), the sphere obtained in this step was termed a *sphere of accuracy*. Each triad had six permutations for the order of rotation and hence six JCs. Combining a single triad from the proximal segment with a single triad from the distal segment gave 36 JCs per triad combination, and ${}^6C_3 \times {}^6C_3 = 400$ combinations. For each of the 400 triad combinations the 36 JC locations per triad pair were fitted with individual *spheres of accuracy*.

Part 2

In this step the kinematics of a punch were measured in order to establish if different marker sets performed differently during a dynamic movement. The 36 JC locations associated with each of the 400 triad combinations were calculated for each frame of the punch and were fitted with a 95% *sphere of precision* using the same iterative procedure as in Part 1. However, unlike the sphere of accuracy the sphere of precision was established for each frame throughout the time history of the punch rather than for one static frame. The maximal radius of each sphere of precision obtained during the punch was recorded and then the combination of the proximal and distal triads which resulted in the sphere with the lowest maximal radius was determined. The results of this step could suggest which markers should be used in Part 1 to obtain the most robust estimation of the JC based on the specific athletic activity under investigation.

Part 3

This part aimed to evaluate the variability in JC reconstruction which was associated with triad deformation during two phases of the punch, punch motion (185 samples) and punch impact (65 samples). Three coordinate systems that were as independent as possible but had given good results in Part 2 were selected. The JC location calculated in one of the three triads (S_1 , S_2 or S_3) was expressed in turn in the other two triads. During the punch the change in the vector between the JC and the origin of the two coordinate systems that had not defined the JC was calculated. The maximal change in this vector was an *indicator of the variability*, v_i , in the JC location during the trial. If the segments were rigid and there was no noise, these values should remain constant. This resulted in three simultaneous equations relating variability measured in one coordinate system relative to another coordinate system. The three measured variability indicators are given by the following equations in which a, b and c are the errors associated with S_1 , S_2 and S_3 respectively.

$$v_1 = aS_1 + bS_2 \quad (1)$$

$$v_2 = aS_1 + cS_3 \quad (2)$$

$$v_3 = bS_2 + cS_3 \quad (3)$$

Solving these for the measured error values gives the variability associated with each coordinate system.

The variability in JC location had to be determined in this way for the following reasons. Firstly, due to the measured motion being caused by the true movement of the segment and the movement artefact of the markers, an absolute comparison cannot be made and local systems need to be used. In each local system, the local JC vector was constant but all local coordinate frames deformed and moved during the punch and hence the location of JC vectors relative to the segment would vary but not with respect to their origins. Variability in the real JC location relative to the system origin are not expressible in that system even though they exist. These variabilities can only be noticed by their effect on markers not of their system, but these other markers also have their own variability associated with them. A description of the change between the two independent frames could illustrate the variability of the JC position

RESULTS

All joint centre locations for the shoulder and elbow joints are shown in Figure 2. These clouds of points are made up of overlapping clusters of points relating to the 95% of the 400 triad pairs. As outlined earlier, the JC were reconstructed with solidification (WS) and without solidification (WOS). Table 1 shows the mean x, y, z location of the centre of the sphere for all the JCs and the mean x, y, z location for nine JCs made by combining the best three proximal triads with the best three distal triads. The radius of the best nine WOS was 12 mm and the dispersion, as described by the SD, of the best nine JCs was around 10 mm. Table 1 also shows that although solidification may lower the radii of the best triads, it disperses them more in space as demonstrated in Figure 3.

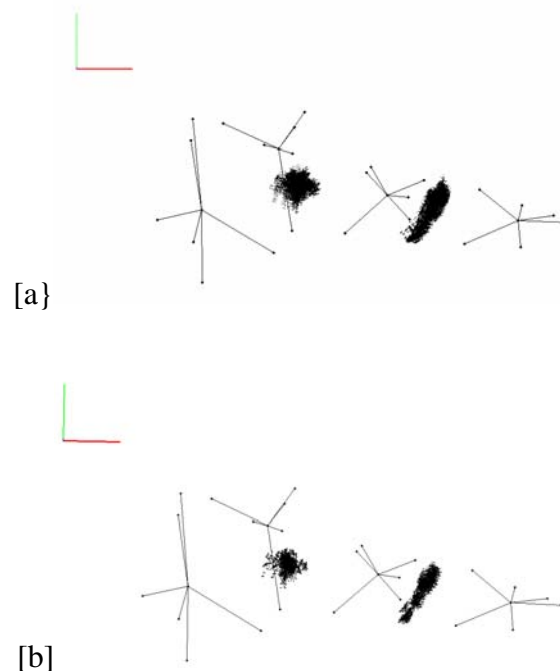


Figure 2: Upper views of the upper limb and the 14,400 locations of shoulder and elbow joint centres (in black dots) without solidification [a] and with solidification [b]. The bodies are from the left to the right: trunk, shoulder, upper-arm and lower arm.

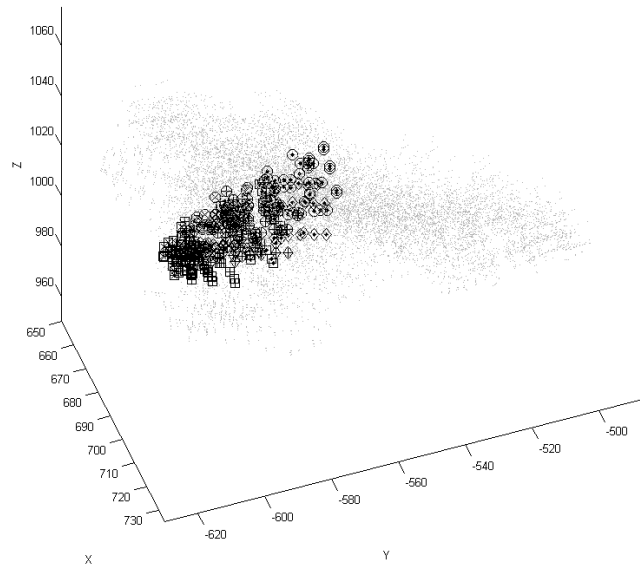
Table 1. Mean x, y, z location of the centre of the sphere for all the JCs and the mean x, y, z location for the best nine JCs for the shoulder (pT₁₅₆, pT₂₄₆, pT₃₄₆ – dT₁₃₅, dT₁₂₃, dT₁₃₄) and elbows (pT₃₄₅, pT₂₄₅, pT₁₃₄ – dT₁₂₅, dT₁₃₄, dT₂₃₄). a – with solidification and b – without solidification.

[a]

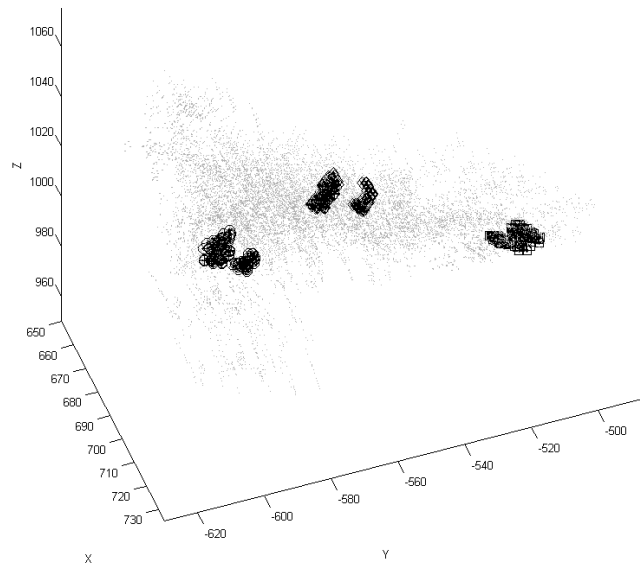
	Without Solidification (mm)							
	Elbow				Shoulder			
	x	y	z	r	x	y	z	r
All points	691.5	573.1	1001.1	74.3	570.6	475.0	1259.3	53.2
Mean, best 9 Ts	696.2	594.3	1018.6	12.3	580.8	469.6	1265.5	11.9
S.D., best 9 Ts	5.4	13.7	3.5	1.6	15.7	10.7	8.8	1.7

[b]

	With Solidification (mm)							
	Elbow				Shoulder			
	x	y	z	r	x	y	z	r
All points	687.5	564.7	1004.2	67.2	570.8	476.1	1260.7	50.8
Mean, best 9 Ts	689.7	554.9	998.7	3.9	589.0	477.2	1258.8	5.5
S.D., best 9 Ts	5.9	40.0	21.2	0.7	20.1	8.3	14.6	0.4



[a]



[b]

Figure 3: A 3D representation of all joint centres (grey) and the joint centres of the best triads for the elbow (black) [a] without solidification and [b] with solidification.

The maximum radii of the *spheres of accuracy* for the 400 JC locations determined without solidification for the shoulder in the static position are shown in Table 2. Figure 4 graphically represents the data format of Table 2 using a 20 by 20 greyscale coded grid; white represents 0 mm and black represents 60 mm. The radii for both the shoulder and the elbow, with and without solidification, are presented in Figure 4.

Table 2: Radii [mm] of the *spheres of accuracy* for the shoulder without solidification. For each couple of proximal - distal triads, the sphere includes 95% of the 36 joint centre locations.

M		1	2	3	1	3	1	1	3	2	1	2	1	1	4	1	1	1	2	2	2	
	M	5	4	4	2	5	2	2	4	4	4	3	4	3	5	3	2	3	5	3	3	
		M	6	6	6	6	6	4	5	5	5	4	6	5	6	6	3	4	6	6	5	
1	3	5	7.6	6.6	7.2	6.7	8.6	11.	11.	12.	12.	13.	13.	14.	16.	15.	16.	16.	17.	18.	20.	22.
1	2	3	8.5	5.7	6.2	7.4	8.5	8.9	12.	11.	13.	14.	14.	15.	16.	15.	17.	17.	18.	18.	21.	24.
1	3	4	10.	6.7	6.9	8.8	8.3	10.	13.	12.	14.	15.	15.	17.	17.	15.	19.	18.	20.	17.	21.	24.
2	3	5	9.7	7.8	8.7	8.6	9.9	12.	12.	13.	14.	16.	15.	16.	17.	18.	17.	18.	19.	19.	22.	26.
1	5	6	10.	8.6	9.9	9.3	10.	13.	14.	14.	15.	16.	15.	17.	18.	17.	18.	19.	20.	20.	21.	24.
3	5	6	9.8	8.1	9.4	10.	10.	12.	16.	14.	16.	15.	15.	16.	17.	19.	18.	20.	19.	20.	23.	25.
1	2	5	9.0	10.	11.	10.	10.	13.	13.	15.	16.	16.	17.	16.	17.	19.	18.	18.	19.	20.	21.	24.
2	5	6	10.	7.6	10.	8.9	10.	13.	14.	15.	15.	17.	14.	17.	17.	20.	19.	19.	20.	20.	23.	26.
1	3	6	10.	9.6	10.	10.	11.	14.	14.	14.	15.	16.	16.	17.	18.	18.	19.	20.	20.	20.	22.	24.
1	4	6	10.	10.	11.	10.	12.	13.	14.	15.	16.	17.	18.	19.	19.	16.	19.	21.	22.	21.	24.	27.
2	3	6	12.	11.	10.	11.	12.	13.	16.	17.	17.	16.	17.	17.	20.	19.	21.	20.	21.	22.	25.	26.
1	2	4	12.	10.	10.	13.	12.	13.	17.	14.	18.	17.	17.	17.	19.	20.	22.	21.	22.	21.	22.	28.
3	4	6	12.	13.	12.	12.	15.	14.	16.	16.	18.	17.	18.	19.	20.	18.	20.	21.	23.	26.	29.	30.
1	2	6	13.	14.	15.	14.	14.	17.	17.	19.	19.	19.	22.	20.	20.	23.	20.	21.	21.	23.	24.	26.
2	3	4	12.	15.	13.	15.	15.	15.	17.	17.	20.	19.	19.	18.	18.	23.	21.	24.	22.	25.	28.	30.
2	4	6	13.	13.	13.	14.	15.	16.	18.	18.	18.	19.	20.	20.	22.	20.	22.	23.	23.	26.	29.	29.
2	4	5	14.	17.	16.	18.	17.	19.	21.	19.	22.	23.	21.	24.	24.	25.	23.	25.	25.	25.	28.	32.
1	4	5	14.	18.	16.	19.	18.	21.	20.	20.	24.	21.	22.	23.	25.	23.	21.	25.	25.	27.	28.	29.
4	5	6	14.	16.	15.	19.	17.	21.	22.	21.	24.	22.	22.	24.	26.	24.	22.	27.	25.	25.	28.	30.
3	4	5	16.	20.	18.	20.	19.	21.	20.	23.	24.	24.	23.	23.	25.	27.	25.	26.	25.	27.	28.	32.

Note: The local frames were calculated with markers M1, M2 and M3. M1-M2 defined the x -vector and M1-M2-M3 was the plane of reference.

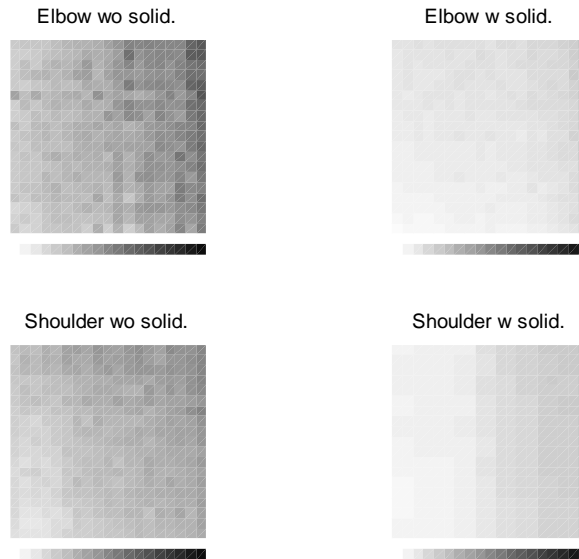


Figure 4: Radii of the sphere of accuracy (static position) for the elbow and the shoulder with (w solid.) and without (wo solid.) solidification.

Note: the linear colour code represents the radius (white=0 mm and black=60 mm). The bottom left figure (*Shoulder wo solid.*) is a representation of Table 2. The results were sorted in rows and columns according to the average value of the proximal and distal triads. This means the bottom left Figure 2 is equal to the top left of Table 2.

The JC locations for the shoulder and elbow joints are shown in Figure 5. The maximum radii of the *spheres of precision* of the 36 JC locations throughout the punch are shown in Figure 6 (same graphical parameters as Figure 4). During the punch the maximum radii for the shoulder ranged from 13.5 to 43.3 mm WOS and from 6.2 to 24.6 mm WS; the maximum radii for the elbow ranged from 14.0 to 55.6 mm WOS and from 3.0 to 23.8 mm WS. The best ten triad pairings are in Table 3 and show that not all triads that performed well in Part 1 did so in Part 2.

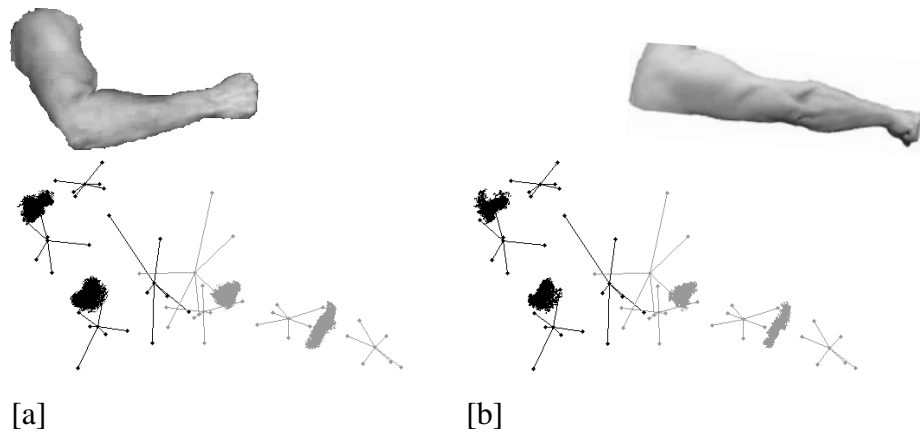


Figure 5: Lateral views of the upper limb and the 14,400 locations of shoulder and elbow joint centres without solidification [a] and with solidification [b] for the 1st frame (black lines and dots) and the 220th frame (grey lines and dots) of the punch. Approximate arm position for the 1st frame is in [a] and for the 220th frame in [b].

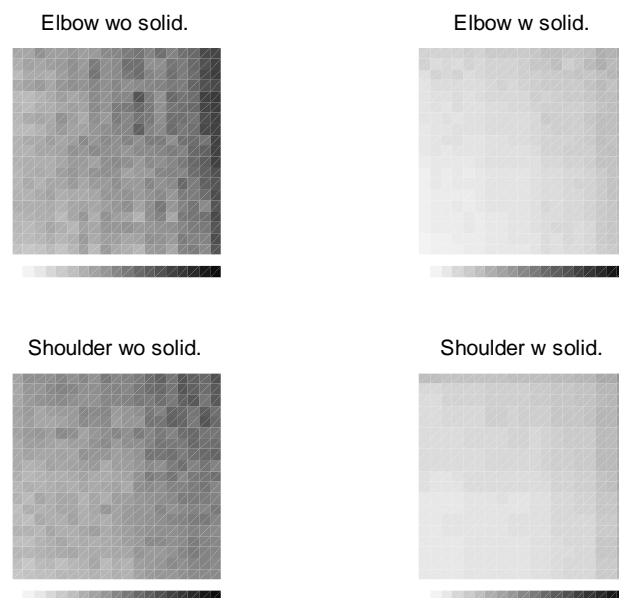


Figure 6: Radii of the sphere of precision (during the movement) for the elbow and the shoulder with (w solid.) and without (wo solid.) solidification.

Note: the linear colour code represents the radius (white=0 mm and black=60 mm). The results were sorted in rows and columns according to the average value of the proximal and distal triads.

Table 3: Radii [mm] of the *spheres of precision* for the ten best triads for the shoulder, without solidification. For each couple of proximal - distal triads, the sphere includes 95% of the 36 joint centre locations.

M1			1	1	3	1	1	1	1	4	2	1
	M2		5	2	4	4	2	4	2	5	4	3
		M3	6	6	6	6	4	5	5	6	6	4
1	3	5	13.5	14.3	15.8	15.7	17.3	17.7	17.4	18.7	17.6	19.2
1	2	3	15.7	13.8	16.3	17.3	15.1	17.3	18.4	21.1	16.7	19.5
2	3	5	17.0	17.6	18.3	19.4	20.0	21.5	18.8	19.8	20.5	21.2
3	5	6	15.9	15.5	18.7	19.3	21.2	19.4	20.0	19.4	20.2	21.5
1	3	6	18.6	18.6	17.7	21.1	19.4	19.3	21.4	23.3	19.7	22.0
2	5	6	16.8	15.6	20.0	18.8	19.3	22.4	19.0	20.2	19.0	22.4
1	2	5	15.5	19.6	18.7	19.5	21.5	21.1	19.2	20.9	24.6	22.1
1	5	6	18.0	16.7	21.0	19.4	21.4	21.1	18.7	21.2	19.4	22.7
2	3	6	17.1	19.2	18.7	19.5	20.0	19.1	21.3	20.4	20.7	22.3
1	3	4	19.3	17.1	18.6	19.0	19.1	20.0	22.0	19.8	20.6	21.5

The variability associated with the different co-ordinate systems is shown in Table 4. The table shows the variability per marker set on the proximal and the distal segment for punch motion and punch impact and only WS. For the shoulder the variability ranges from 2.5 to 13.8 mm for the punch motion and from 8.2 to 31.2 mm for the punch impact. For the elbow the variability ranges from 1.5 to 21.1 mm for the punch motion and from 4.8 to 72.4 mm for the punch impact.

Table 4: Indicators of variability in the joint centre ([a] shoulder and [b] elbow) reconstruction due to the triad deformation during the movement and the impact for the proximal and the distal segments. (T = triad)

[a]

SHOULDER JC with solidification						
	Precision	Markers			Movement (mm)	Impact (mm)
SHOUL.	T1	1	4	5	9.1	12.9
	T2	3	4	6	10.0	31.2
	T4	1	2	3	4.3	8.3
U. ARM	T1	4	5	6	13.8	23.9
	T3	1	2	5	2.5	26.6
	T5	1	3	4	12.4	8.2

[b]

ELBOW JC with solidification						
	Precision	Markers			Movement (mm)	Impact (mm)
U. ARM	T3	4	5	6	5.6	13.0
	T4	1	3	6	2.4	8.6
	T7	1	2	5	20.2	58.1
L. ARM	T1	3	4	6	21.1	72.4
	T2	2	4	5	19.0	57.1
	T3	1	2	3	1.5	4.8

DISCUSSION

Although the functional methods by Ehrig et al. (2006) have produced very accurate results in estimating JC in theory ($< 1\text{mm}$), additional problems introduced and further steps required when determining and utilising JC with human movement data decreased this accuracy considerably. Part 1 involved determining the JC locations but nowhere near the accuracy reported by Ehrig et al. (2006) was possible even using the most optimistic results from this study. The radii of the spheres of all the points includes triads which would be expected to perform poorly so gives an unrealistic worst case scenario for the spread of possible JCs. Ninety-five percent of a population lies within two SD, and the SD of the mean JC of the best nine JCs was 10 mm. Combining this with the diameter of an individual triad's JCs being 24mm, these results would indicate that determining the JC with an accuracy of greater than 20 mm is unlikely. This value is more comparable with the 13 mm RMS error found by Leardini et al. (1999) in the location of the hip JC using functional methods with a stereophotogrammetric reference.

Although radii in Table 1 are lower with solidification, they have limited importance in Part 1 as they only illustrate the precision of each individual group of JCs for a triad, not how well they group together about a single point in space. Hence, it does not give any information about whether there may be a degree of consistency in finding a real point that is comparable to the real JC. For both the shoulder and the elbow, although precision increased, the spread of the JCs in space for the well behaved triads was worse. Although solidification has reduced random error it has dispersed the precise groups further apart, especially along one axis of the elbow. This is likely to be a result of systematic errors introduced from skin movement artefact which is not random but has its own coherent structure (Pain & Challis, 2002) and is often correlated with the whole limb motion (Woltring, 1991). The elbow exhibited this effect more severely than the shoulder with the results distributed along an axis and solidification dispersed JCs along this axis. This was more prominent with the arm extended than with the arm flexed.

Although the elbow was modelled as a ball and socket joint, this is not due to a single physiological joint complex but combines the two components of motion at the elbow joint with potential humeral rotation not expressed on the upper arm. Given that the motion normally associated with the elbow joint is itself a combination of two movements about different axes, and actually two different 'joints', adding a third component in order to examine the viability of the technique seems justifiable. If the humeral rotation not expressed on the upper arm markers is along a single axis, that does not translate relative to the elbow joint, the location of the JC should be determinable for the composite joint. With the elbow extended to around 180 degrees the humeral rotation will be near a singularity with the pronation-supination of the forearm and is likely to cause additional problems. The pronation-supination was subject to very large skin movement artefact for many markers, and was clearly visible with the naked eye. It is likely that a combination of problems with accurately defining a single elbow joint centre, skin movement artefact, and singularities near elbow extension contribute to the relatively poor elbow results, especially near extension. Proximal markers on the forearm will not have provided sufficient pronation-supination information and hence resulted in JC locations on the axis of rotation.

In order to choose the optimal marker set for the athletic activity which is to be studied, this paper suggest conducting a pilot study in which the athletic movement is studied carefully to obtain a *sphere of precision* for various marker triads. One of the triads yielding the smallest radii should be chosen to conduct the set-up movements to determine the JC for this particular activity. It was not expected that the best triads

found in Part 2 would always be the same as the best triads found in Part 1, since the movement artefact of the markers in the set-up movements was unlikely to be the same as that in the actual dynamic activity. This is confirmed by the results. The best spheres of accuracy and precision are often based on the same markers but not always. It has previously been shown that skin movement artefact is subject and task dependent (Leardini et al., 2005) and as it stands the results of this study need to be addressed with this in mind; hence the suggestion of carrying out a pilot study to determine suitable markers. As the databases of movements and associated movement artefacts expand it is hoped that more generic principles may be determined in the future. For Parts 2 and 3 using solidification to determine the spheres of precision was a great benefit as a triad that did not vary during the movement is required to accurately determine whatever location has been defined as the JC.

After having determined the JC in terms of a marker set that does not vary excessively during the activity, it was important to quantify how reliable this location was during the activity. Hence, the JC – triad origin vector was compared in two other co-ordinate systems and simultaneous equations were solved to give an indicator of the variability of each co-ordinate system in which the JC could be reconstructed and this was done for a few different triads. Reconstructing a JC from a single set of markers is likely to adversely affect the results. The same markers on a segment tend to perform well. Hence, it is difficult to pick good triads which are completely independent. It should also be noticed that different triads performed well during the movement and impact phase of the punch, hence highlighting the soft tissue motion dependence. The implementation of a solidification procedure makes a marked difference.

The major limitation of the study is that a true gold standard JC was not determined for comparative purposes and if the best performing triads, by any measure, have a systematic offset then all inferences may be impugned. However, the theory and application of the methodologies would still be valid and could be extrapolated to any type of virtual markers (to avoid occlusions or drop offs). In this case it will still be possible to calculate the expected variability but no gold standard would exist.

In conclusion, this research suggests that markers used to determine the JC using the functional method should be chosen specifically for the activity under investigation. The best accuracy obtained in JC determination will not be as accurate as that found in theoretical settings and will be on the order of tens of millimetres. Further inaccuracies on the order of a few millimetres to tens of millimetres will be introduced by the reconstruction of the estimated JC due to marker motion used to define the JC during the activities.

REFERENCES

- Andriacchi, T.P., Alexander, E.J., Toney, M.K., Dyrby, C. & Sum, J. (1998). A point cluster method for in vivo motion analysis: applied to a study of knee kinematics. *Journal of Biomechanical Engineering*, 120, 743-749.
- Bao, H. & Willems, P.Y. (1999). On the kinematic modelling and the parameter estimation of the human shoulder. *Journal of Biomechanics*, 32, 943-950.
- Begon, M., Monnet T. & Lacouture, P. (2007). Effects of movement for estimating the hip joint centre. *Gait & Posture*, 25, 353-359.
- Bell, A.L., Pedersen, D.R. & Brand, R.A. (1990). A comparison of the accuracy of several hip center location prediction methods. *Journal of Biomechanics*, 23, 617-621.

- Camomilla, V., Cereatti, A., Vannozzi, G. & Cappozzo, A. (2006). An optimised protocol for hip joint centre determination using the functional method. *Journal of Biomechanics*, 39, 1096-1106.
- Cappozzo, A., Catani, F., Leardini, A., Benedetti, M. & Croce, U.D. (1996). Position and orientation in space of bones during movement: experimental artefacts. *Clinical Biomechanics*, 11, 90-100.
- Challis, J.H. (1995). A procedure for determining rigid body transformation parameters. *Journal of Biomechanics*, 28, 733-737.
- Chèze, L., Fregly, B.J. & Dimnet, J. (1995). A solidification procedure to facilitate kinematic analyses based on video system data. *Journal of Biomechanics*, 28, 879-884.
- De Leva, P. (1996). Joint center longitudinal positions computed from a selected subset of Chandler's data. *Journal of biomechanics*, 29, 1231-1233.
- Ehrig, R. M., Taylor, W. R., Duda, G. N. & Heller, M. O. (2006). A survey of formal methods for determining the centre of rotation of ball joints. *Journal of Biomechanics*, 39, 2798-2809.
- Karlsson, D. & Lundberg, A. (1994). Accuracy estimation of kinematic data derived from bone anchored external markers. In *Proceedings of the 3rd International Symposium on 3-D Analysis of Human Motion. Stockholm, Sweden.*
- Leardini, A., Cappozzo, A., Catani, F., Toksvig-Larsen, S., Pettitto, A., Sforza, V., Cassanelli, G. & Giannini, S. (1999). Validation of a functional method for the estimation of hip joint centre location. *Journal of Biomechanics*, 32, 99-103.
- Monnet, T., Desailly, E., Begon, M., Vallée, C. & Lacouture, P. (2007). Comparison of the SCoRE and HA methods for locating *in vivo* the glenohumeral joint centre. *Journal of Biomechanics*, 40, 3487-3492.
- Pain, M.T.G. & Challis, J.H., 2002. Soft tissue motion during impacts: their potential contribution to energy dissipation. *Journal of Applied Biomechanics*, 18, 231-242.
- Piazza, S.J., Erdemir, A., Okita, N. & Cavanagh, P.R. (2004). Assessment of the functional method of hip joint center location subject to reduced range of hip motion. *Journal of Biomechanics*, 37, 349-356.
- Piazza, S.J., Okita, N. & Cavanagh, P.R. (2001). Accuracy of the functional method of hip joint center location: effects of limited motion and varied implementation. *Journal of Biomechanics*, 34, 967-973.
- Reinschmidt, C., Bogert, A., Nigg, B., Lundberg, A. & Murphy, N. (1997). Effect of skin movement on the analysis of skeletal knee joint motion during running. *Journal of Biomechanics*, 30, 729-732.
- Sati, M., de Guise, J. & Drouin, G. (1994). In vivo non-invasive 3D knee kinematics measurement and animation system: accuracy evaluation. In *Proceedings of the 3rd International Symposium on 3-D Analysis of Human Motion. Stockholm, Sweden.*
- Shea, K.M., Lenhoff, M.W., Otis, J.C. & Backus, S.I. (1997). Validation of a method for location of the hip joint center. Proceedings of the Second Annual Gait and Clinical Movement Analysis Meeting. *Gait & Posture*, 5, 157-158.
- Siston, R.A. & Delp, S.L. (2006). Evaluation of a new algorithm to determine the hip joint center. *Journal of Biomechanics*, 39, 125-130.
- Woltring, H.J. (1991). Representation and calculation of 3-D joint movement. *Human Movement Sciences*, 10, 603-616.

APPENDICES

Part 1:

Purpose:

1. Calculate JC with Ehrig et al.(2006)'s functional method from all the combinations of 3 markers among 6 fixed on the proximal segment and 3 among 6 on the distal segment. The location is calculated in both local coordinate systems.
2. Calculate the radii of the *sphere of accuracy* for each couple of proximal/distal triads in the global coordinate system for a static posture.

Input:

P (*Positions of the 12 markers in the global frame during the set-up*)

S (*Positions of the 12 markers in the global frame during the static posture*)

Output: **CoR** (*Joint centre locations*), **r1** (*radii of the spheres of accuracy*)

BEGIN

FOR i (*triad of the proximal segment*) \leftarrow 1 to 20

M1 \leftarrow *SelectMarkers*(**P**, i)

FOR k (*triad of the distal segment*) \leftarrow 1 to 20

M2 \leftarrow *SelectMarkers*(**P**, k)

FOR j (*Coordinate system of the triad i *) \leftarrow 1 to 6

R1 \leftarrow *RotationMatrix*(**M1**, j)

FOR l (*Coordinate system of the triad k *) \leftarrow 1 to 6

R2 \leftarrow *RotationMatrix*(**M2**, l)

${}^{ij}C_{kl}^{ij}, {}^{kl}C_{kl}^{ij} \leftarrow$ *LocalCoR*(**M1**, **M2**, **R1**, **R2**)

CoR ${}_{kl}^{ij} \leftarrow$ *GlobalCoR*(${}^{ij}C_{kl}^{ij}, {}^{kl}C_{kl}^{ij}$, **S**)

ENDFOR

ENDFOR

r1 ${}_k^i \leftarrow$ *SphereRadius*(**CoR** ${}_{kl}^{ij}$)

ENDFOR

ENDFOR

END

Part 2:

Purpose:

Calculate the maximal radii of the *spheres of precision* for each couple of proximal/distal triads in the global coordinate system during a punch.

Input:

C (*Centre of rotation locations in all the local frames (Part 1)*)

M (*Positions of the 12 markers in the global frame during the punch*)

Output: r2 (*maximal radii of the sphere of precision*)

BEGIN

FOR i (*triad of the proximal segment*) \leftarrow 1 to 20

FOR k (*triad of the distal segment*) \leftarrow 1 to 20

FOR j (*Coordinate system of the triad i^* *) \leftarrow 1 to 6 [J]

FOR l (*Coordinate system of the triad k^* *) \leftarrow 1 to 6 [K]

FOR t (*samples of the punch*) \leftarrow 1 to T

$\mathbf{CoR}_{kl}^{ij}(t) \leftarrow \text{GlobalCoR}(^j C_{kl}^{ij}, ^k C_{kl}^{ij}, \mathbf{M})$

ENDFOR

ENDFOR

ENDFOR

$r_k^i \leftarrow \text{SphereRadius}(\mathbf{CoR}_{kl}^{ij}(t))$

$\mathbf{r2}_k^i \leftarrow \max(r_k^i)$

ENDFOR

ENDFOR

END

Part 3:

Purpose:

Calculate the variability of the JC location during an athletic movement due to proximal (or distal) triad deformation for the three best and as independent as possible triads that were defined in part 2:

1. Express the JC calculated from one triad in the other two triads for the punch before and during impact
2. Calculate the maximal distance between the JC vector relative to the average vector
3. Solve a linear system to determine the variability associated to the three triads

Algorithm for the proximal segment

Input:

C (*Centre of rotation locations in local frame for 3 proximal and 3 distal triads (Part 1)*)

S (*Markers positions in the global frame during the static posture*)

M1 (*Markers positions in the global frame before impact*)

M2 (*Markers positions in the global frame during the impact*)

Output:

L1 (*maximal change in position of the JC before impact*)

L2 (*maximal change in position of the JC during the impact*)

V1 (*variability due to triad deformation before impact *)

V2 (*variability due to triad deformation during impact*)

BEGIN

FOR i (*best triad for the proximal segment*) \leftarrow 1 to 3 [I]

FOR $i2$ (*other best triad for the proximal segment*) \leftarrow 1 to 3 [I2]

FOR j (*Coordinate system of the triad i^*) \leftarrow 1 to 6 [J]

$\mathbf{mCoR}^{ij} \leftarrow \text{MeanLocalCoR}(^{ij}C_{KL}^{ij}, {}^{KL}C_{KL}^{ij}, \mathbf{S})$

FOR t (*samples before impact*) \leftarrow 1 to T1

$\mathbf{CoR1}^{ij}(t) \leftarrow \text{GlobalCoR}(\mathbf{mCoR}^{ij}, \mathbf{M1})$

ENDFOR

FOR t (*samples during impact*) \leftarrow 1 to T2

$\mathbf{CoR2}^{ij}(t) \leftarrow \text{GlobalCoR}(\mathbf{mCoR}^{ij}, \mathbf{M2})$

ENDFOR

FOR $j2$ (*Coordinate system of the triad $i2^*$) \leftarrow 1 to 6 [J2]

```

FOR  $t$  (*samples before impact*)  $\leftarrow$  1 to T1
   ${}^{ij}\mathbf{CoR1}^{i2j2}(t) \leftarrow LocalCoR(\mathbf{CoR1}^{ij}, \mathbf{M1})$ 
ENDFOR
FOR  $t$  (*samples during impact*)  $\leftarrow$  1 to T2
   ${}^{ij}\mathbf{CoR2}^{i2j2}(t) \leftarrow LocalCoR(\mathbf{CoR2}^{ij}, \mathbf{M2})$ 
ENDFOR

 ${}^{ij}\mathbf{D1}^{i2j2} \leftarrow DistanceToAverage(\mathbf{CoR1}^{i2j2}_{KL})$ 
 ${}^{ij}\mathbf{D2}^{i2j2} \leftarrow DistanceToAverage(\mathbf{CoR2}^{i2j2}_{KL})$ 
ENDFOR
ENDFOR

 ${}^i\mathbf{L1}^{i2} \leftarrow MaxError({}^{ij}\mathbf{D1}^{i2j2})$ 
 ${}^i\mathbf{L2}^{i2} \leftarrow MaxError({}^{ij}\mathbf{D2}^{i2j2})$ 

ENDFOR
ENDFOR

 $\mathbf{V1} \leftarrow SolveLinearEq({}^i\mathbf{L1}^{i2})$ 
 $\mathbf{V2} \leftarrow SolveLinearEq({}^i\mathbf{L2}^{i2})$ 

END

```